Journal of Hydroscience and Hydraulic Engineering
Vol. 25, No.1 May, 2007, 11-20

TOWARDS THE DEVELOPMENT OF A LAND DATA ASSIMILATION SYSTEM FOR SNOW

By

Tobias GRAF,

Department of Civil Engineering, University of Tokyo, Bunkyo-ku, Tokyo, Japan

Toshio KOIKE

Department of Civil Engineering, University of Tokyo, Bunkyo-ku, Tokyo, Japan

and

Hideyuki FUJII

Department of Civil Engineering, University of Tokyo, Bunkyo-ku, Tokyo, Japan

SYNOPSIS

The present paper introduces the first steps towards the development of a land data assimilation system for snow, based on the assimilation of passive microwave brightness temperature (TB) observations. It introduces the coupling of a land surface model used by the Japanese Meteorological Agency (JMA) and a radiative transfer model for snow. In the first stage, JMA-SiB was extended to predict the change of the snow grain during the winter season, which has a significant impact on the TB observation and the radiative transfer in snow. The model results indicate, that the new version is capable of predicting the snow grain size. Furthermore, as a preliminary a version of the coupled system was applied to data observed during the Cold Land Processes Field Experiment (CLPX) in Boulder Colorado (2003), to assimilate the TB change at 89 GHz after snowfall events and the results agreed with the observed change of the snow water equivalent at the site.

INTRODUCTION

Snow plays an important role in the global energy and water balance, e.g. snow changes the runoff characteristics of a catchment and influences the soil moisture and evaporation (1), due to the high albedo and thermal insulation of snow. Up to 53% of the northern hemisphere and up to 44% of the world land mass can be covered with snow at any given time (2) and world wide one third of the water used for irrigation is temporarily stored as snow (3).

The Climate and Cryosphere (CliC) Project stated that knowledge of the amount, distribution, and type of precipitation and its temporal and spatial variability on a wide range of scales is essential for the study of cold climate and related hydrological processes (4).

To increase the temporal and spatial resolution of snow data, several approaches are possible. Passive microwave

remote sensing observations are sensitive to the size and number of snow particles and, therefore, provide information about the current snow pack conditions. This information is used in the current satellite algorithms to estimate the snow depth or the snow water equivalent (SWE)(5). If meteorological forcing data are available, e.g. from observations or in the form of model output, it is also possible to use a snow model or a land-surface scheme to predict the evolution of the snow cover.

Both approaches have drawbacks. Current satellite snow products do not consider the effect of snow metamorphism and the snow models do not consider the instability of long-term model runs due to the accumulation of model errors or inaccurate initial conditions. Furthermore, in case of a forward modeling approach, accurate forcing data is necessary, especially the amount of precipitation is a very important input parameter.

In this paper the first steps towards the development of a land data assimilation system are introduced, which tries to combine the merits of satellite observations and forward models. This paper also focuses on the extension of JMA-SiB (Japanese Meteorological Agency - Simple Biosphere Model) to consider snow grain metamorphism, which affects the calculation of the radiative transfer in snow. The land surface scheme is then coupled with a radiative transfer model. The coupled system is applied to data collected during the Cold Land Processes Experiment (CLPX) for the assimilation of new snow on the ground (6).

METHODOLOGY

Data Assimilation

Brightness temperature (TB) observations in the microwave region are sensitive to snow on the ground. This is mainly due to the scattering effect of the snow particles, which is determined by the number and size of the particles. Therefore, the TB observations provide information about the state of the snow pack. The basic idea of data assimilation is to repeatedly introduce information into a land-surface or a snow model to generate improved initial conditions for the model run.

Fig. 1 provides a general overview of the assimilation process. The snow model, which is called the model operator, is used with observed forcing data and initial conditions as input to predict the evolution of a snow cover until new radiometer observations are available (from T_0 to T_1). The predicted snow pack state is then used as input parameter for the radiative transfer model (RTM), which is called the observation operator.

The observation operator calculates the brightness temperature for the predicted snow pack structure at T_1, which would be observed by a radiometer and compares this result with the observed brightness temperature using a cost function. By changing the initial conditions of the model operator in a predefined range, this step will be repeated until the estimated and observed brightness temperatures are in close agreement. Because this methodology describes a variational approach, which changes the initial condition and the forcing data at T_0, the assimilation system restarts from the original time point ($T = T_0$), until the cost function is minimized. To minimize the cost function of this algorithm the shuffled complex evolution method (SCE) is introduced. The parameter range of the initial condition can for example be decided based on

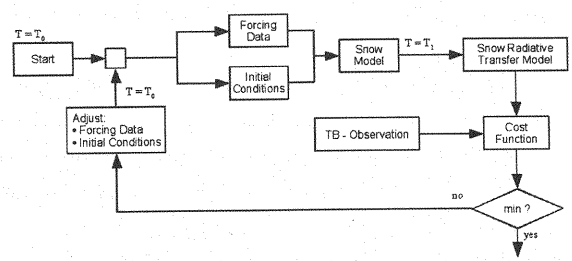

Fig. 1 Flowchart of the general data assimilation approach.

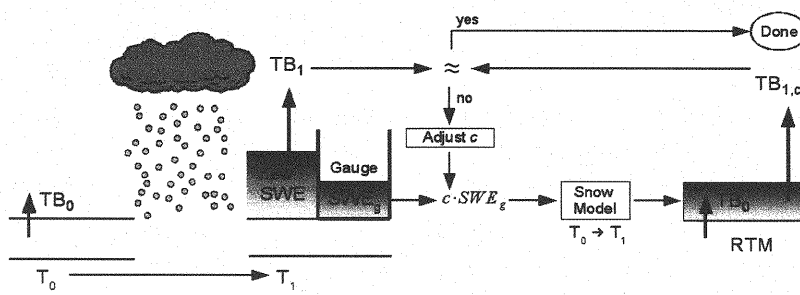

Fig. 2 Flowchart to assimilate the TB change at 89 GHz to estimate the new snow amount.

the variance of the parameter. The variance can be determined from experience and/or historical data.

Similar approaches have been used successfully to assimilate passive microwave satellite observation to determine the spatial and temporal variation of soil moisture and soil temperature (7).

New Snow Assimilation

To begin with, we implemented an approach to assimilate the change of brightness temperature observations at 89 GHz to estimate the amount of new snow on the ground (6). This is done by correcting the observed data from a precipitation gauge, which often only catches a fraction of the actual precipitation, due to wind-induced under-catch or evaporation.

The brightness temperature at 89 GHz shows a high sensitivity to the amount of fresh snow on the ground. Therefore, it is possible to relate the change in the brightness temperatures at this frequency between two different times (T_0 and T_1) to the accumulated new snow. The advantage of this algorithm is that it is not necessary to know the physical properties of the old snow. In addition, the fresh snow on the ground is assumed to have a homogeneous vertical profile, which further simplifies the problem.

Fig. 2 provides an overview of the algorithm. The figure shows a snowpack (T_0) for which the brightness temperature (TB_0) was observed. After the snowfall event (T_1) a new brightness temperature (TB_1) is observed, which includes the actual amount of new snow (SWE). Afterwards the gauge data (SWE_g) and the first guess of the correction factor (c) are input parameters for the snow model (T_0 to T_1). The results of the snow model and the brightness temperature for the old snow (TB_0) are then used to calculate the radiative transfer in the fresh snow. The results of the radiative transfer model ($TB_{1,c}$) are then compared with the observed brightness temperature (TB_1). During the assimilation process, the correction factor for the observed solid precipitation is updated until $TB_{1,c}$ is in good agreement with TB_1.

An important assumption in this algorithm is that TB_0 does not change between the two observations (T_0 and T_1). Snow grain size, density and temperature are parameters which can influence the brightness temperature. We assume that the change in the grain size and the density are small within this time period and, therefore, the effect of their change on TB_0 is negligible. An example of a frequent observation system is the Advanced Microwave Scanning Radiometer (AMSR-E) on board Aqua, which can provide brightness temperature data on a daily basis.

Assimilation of Lower Frequencies

Current passive microwave satellite sensors, e.g. AMSR-E, are providing TB observations at lower frequencies like 18.7 GHz and 36.5 GHz on a daily basis. These frequencies are also sensitive to the snow on the ground, but show only a low sensitivity to fresh snow. Thus, the next step in the development of the land data assimilation scheme will be to introduce TB observations at lower frequencies. In view of this matter, it is necessary to consider longer assimilation steps and, as a result, the effect of the snow grain growth becomes more important and needs to be considered.

Model Operator – JMA-SiB

We selected the new land-surface model developed by JMA as the model operator, called JMA-SiB (8) in this paper. The model is an extension of the Simple Biosphere (SiB) model developed by Sellers et. al. (9). SiB was developed to express the transfer of energy, mass and momentum between the land-surface and the atmosphere, a process in which snow plays an important role. The changes which were introduced are based on experience at JMA with using SiB as part of the global numerical weather prediction model. The changes include the introduction of:

- Multiple Snow Layers; and
- Sophisticated Snow Processes such as aging of albedo, temporal change of density and so on.

The original JMA-SiB does not consider the effects of the snow grain growth which is an important parameter for radiative transfer in snow. We implemented a grain growth model proposed by Rachel Jordan (10). For dry snow, grain growth is estimated based on the temperature gradient:

$$\frac{dr}{dt} = \frac{1}{4}\frac{g_1}{r} D_{eos}\left(\frac{1000}{P_a}\right)\left(\frac{T}{273.15}\right)^6 C_{iT}\left|\frac{dT}{dz}\right| \tag{1}$$

where r represents the mean grain radius, D_{eos} the effective diffusion coefficient of water vapor in snow, C_{iT} the variation of saturation vapor pressure with temperature relative to ice, dT/dz the temperature gradient in the snow pack and g_1 $(=5.0 \cdot 10^{-7} m^4/kg)$ is an empirical parameter.

For wet snow the following equations are used:

$$\frac{dr}{dt} = \frac{1}{4}\frac{g_2}{r}\cdot(\theta_l + 0.05) \;; \qquad \theta_l < 0.09 \tag{2}$$

$$\frac{dr}{dt} = \frac{1}{4}\frac{g_2}{r}\cdot 0.14 \;; \qquad \theta_l \geq 0.09 \tag{3}$$

where g_2 $(=4.0 \cdot 10^{-12} m^2/kg)$ is an empirical coefficient and θ_l the snow wetness.

The initial condition for new snow (precipitation) is set to 0.5 mm.

Observation Operator – MEMLS

The Microwave Emission Model of Layered Snowpack (MEMLS) was used as the observation operator. The model was explicitly developed for radiative transfer modeling in snow and successfully applied (11,12).

MEMLS is a radiative transfer model used to calculate the microwave emission from a layered snow pack. It can calculate the brightness temperature for a given frequency, polarization and incident angle. The snowpack is represented as a stack of homogeneous layers. The model calculates the radiative transfer inside each layer by using the correlation length of the snow, the snow density, temperature and SWE.

MEMLS uses the correlation length and function to represent the spatial distribution of the scattered power and together they both correspond to the size, shape and orientation of the discrete scatterer (snow grains) (13). To be more precise, the correlation function describes the permittivity fluctuation in a medium.

Cost Function

The assimilation scheme is used to minimize the cost function J by adjusting the state vector x (14). In general J can be

separated into two different costs, one represents the background error J_B and the other one the observation error J_0:

$$J = J_B + J_0 \tag{4}$$

For this application, we currently disregard the background error, and only use the observation error J_0, which usually expresses the difference between the observed and modeled values by considering the error covariance matrix R:

$$J(x_0, f) = \frac{1}{2}\sum_{i=1}^{N}\left\{H[M(x_0, f)] - y_i^0\right\}^T R^{-1}\left\{H[M(x_0, f)] - y_i^0\right\} \tag{5}$$

y_i^0 is a vector representing the satellite observation at time i, which will be assimilated. H is the radiative transfer model (observation operator) and R is the error covariance matrix of the observation. M is the model operator, which calculates the model state at i from initial conditions x_0 and forcing data f.

Shuffled-Complex Evolution

During the assimilation the cost function J (Eq. 5) is minimized by adjusting the amount of solid precipitation within one assimilation window. This is done by means of the Shuffled-Complex Evolution method (SCE) (15).

The method involves the evaluation of the function usually at a random sample of points in a feasible parameter space, followed by a subsequent manipulation of the sample using a combination of deterministic and probabilistic rules.

APPLICATION

Dataset from CLPX 3

The data (16, 17) used in this study were obtained during the IOP 3 of the Cold Land Processes Field Experiment (CLPX) at the Local-Scale Observation Site (LSOS) in Fraser, Colorado, USA. The objective of the CLPX was to improve our understanding of the terrestrial cryosphere, using a multi-sensor, multi-scale approach (18).

Within the CLPX the LSOS was used to make very detailed observations of the local snow conditions, soil properties, vegetation and energy balance characteristics, which allow the investigation of scaling issues between ground based observations and airborne-/satellite-based sensors. Hardy et. al. (19) provide a complete overview of all data collected at the LSOS.

The radiometer data were obtained by using a ground based radiometer system from the University of Tokyo (16). It provided observations at 18.7, 36.5 and 89 GHz. The footprint size on the ground was roughly 5.0 m by 2.5 m.

Modeling Results

In this section, the results of the extended version of JMA-SiB will be introduced.

The forcing data set used in this application provides observations between 1 October 2002 and 29 March 2003. Two different cases are presented: for the first case (C1) the model was initialized before the snow accumulation started (Oct. 15); and for the second case (C2) the model was initialized after the first snow pack data was collected on Nov. 13, 2002. The initial parameters were as follows: SWE = 87 mm; Density = 206 kg/m3; and Grain Diameter = 0.5 mm.

For all applications raw precipitation data were used, which did not consider possible losses due to, e.g., wind induced under-catch.

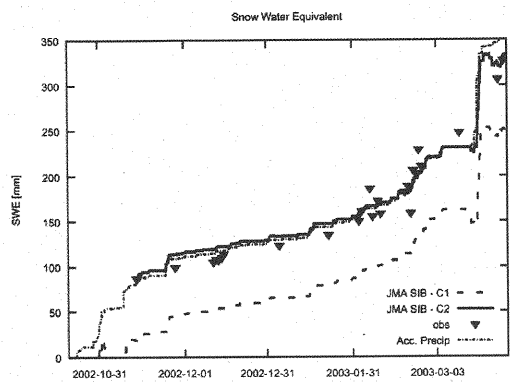

Fig. 3 Model results (SWE) for C1 and C2 and comparison to observed SWE and accumulated precipitation.

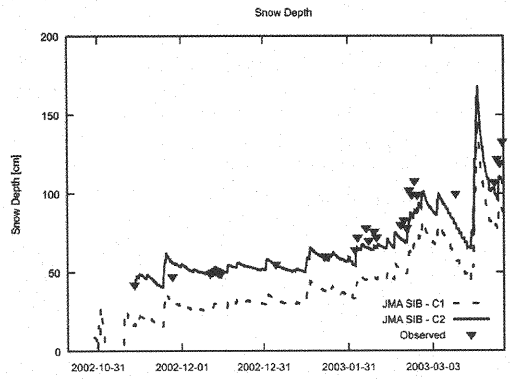

Fig. 4 Model results (Snow Depth) for C1 and C2 and comparison to observed SWE and accumulated Precipitation.

Snow Depth & SWE

Fig. 3 and Fig. 4 show the modeled snow water equivalent (SWE) and snow depth for two different cases and compare the results to observed data. Fig. 3 includes the total accumulated observed precipitation.

For C1 the snow, which accumulated around Oct. 31st, melted at the beginning of November. This error propagates through the results for the entire winter season.

As it can be seen for C2, using the observation data for new (improved) initial conditions significantly improves the model results. The snow depth is represented well by JMA-SiB for the entire winter season. In 2003, the snow depth is somewhat underestimated which is caused by an overestimation of the snow density.

Snow Pack Temperature

Fig. 5 shows a comparison of the snow pack temperature using data from Dec. 13th and Feb. 21st. In both cases, JMA-SiB underestimates the snow pack temperatures; the gap is especially large on Dec. 13th.

The model currently does not consider the effect of the snow micro-structure on the heat transfer in the snow pack (20). This might account for the difference between the modeled and observed snow temperature. In Fraser rather large depth hoar snow crystals are expected, which will reduce the thermal conductivity of the snow cover (21).

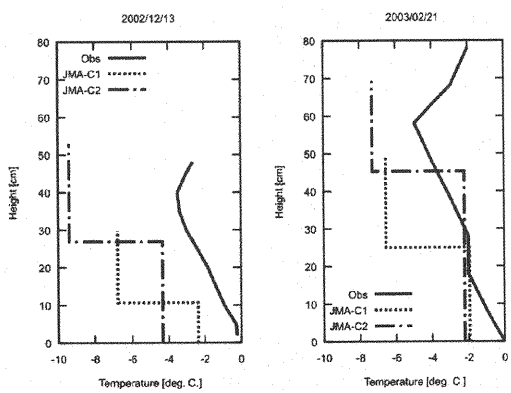

Fig. 5 Temperature profile for C1 and C2 on Dec. 12, 2002 and on Feb. 21, 2003 and comparison with observed profile.

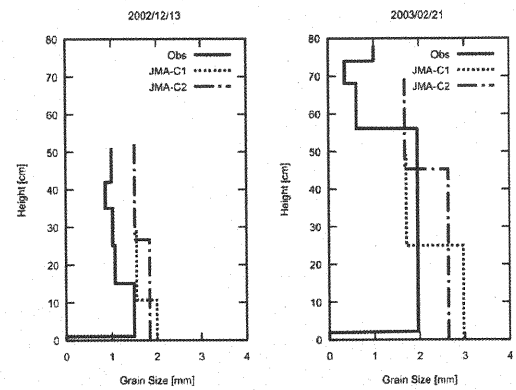

Fig. 6 Snow Grain Size Profile for C1 and C2 on Dec. 12, 2002 and on Feb. 21, 2003 and comparison with observed profile.

Table 1 Observed SWE [mm] and the SWE change [mm] at L1 and L2 and the observed precipitation [mm].

Date	*SWE*		*ΔSWE*		*Precip.*
	L1	L2	L1	L2	
Feb. 19, 12:10		182.0			
Feb. 20, 15:30	189.0				0.0
Feb. 21, 11:30		159.0		-23.0	0.5
Feb. 22, 11:00	206.0		17.0		10.4
Feb. 23, 11:00		203.0		44.0/21.0	4.8
Feb. 24, 13:30	229.0		23.0		4.8
Feb. 25, 11:00		211.0		8.0	3.0

Grain Size

As it can be seen from Fig. 6, the observed and modeled grain sizes are in good agreement, but the model seems to overestimate the snow grain size. Eq. (1) shows the importance of the snow pack temperature for the calculation of the grain growth. Therefore, one reason for the overestimation of the grain size could be the underestimation of the snow pack temperature, which can lead to a larger temperature gradient in the snow cover and therefore to a faster snow grain growth.

Assimilation Results

In this section, the results of the new snow assimilation scheme using radiometer data which were observed during IOP3 of the CLPX are introduced.

The assimilation system runs between Feb. 21, 12:00 and Feb. 25, 14:45. During this period a total of 23 mm snowfall was recorded at the precipitation gauge. The LSOS snow pit data were collected close to the radiometer at two different locations (L1 and L2) and each location was sampled every second day.

The snow pit sites were located in a large forest clearing of the LSOS. The distance between L1 and L2 was about 15 m, but 'L1' was closer to the forest edge, whereas 'L2' was more in the open field (16).

Table 1 provides an overview of the observed SWE for each location and the change between two samples (ΔSWE). The column 'Precip.', indicates the amount of snowfall since the previous day. The data which were used as the initial conditions are marked in gray. During the days before, no snowfall was observed.

Comparing the SWE on Feb. 21st with the one on Feb. 19th (at L2), there seems to be a loss of 23 mm; the only possible explanation for this is a re-allocation of the snow due to strong winds, or an error in sampling the snow pack. If the observation on Feb. 19th is considered as a reference, ΔSWE is 21 mm, rather than 44 mm.

Two different cases were considered for the assimilation. For the first case, the assimilation window was selected to cover one day ('A1'), which includes one set of TB and for the second case the assimilation window was two days ('A2'), including two sets of TB observations.

The results are summarized in Table 2. Because the SWE change between the snow pits can only be compared for the same location, the assimilation results were accumulated to cover the same periods. In Table 2 'A1' and 'A2' correspond to

Table 2 Results for A1 and A2 [mm] compared to the observed SWE change [mm] and the observed Precipitation [mm].

Period	*L2*				*L1*		
	Δ	*A1*	*A2*	*P*	*Δ*	*A1*	*P*
Feb. 21 – 22	44.0/				17.0	22.6	10.4
Feb. 22 – 23	21.0	23.0	23.3	15.2			
Feb. 23 – 24					23.0	14.3	9.6
Feb. 24 – 25	8.0	46.1	37.4	7.8			

the accumulated new snow on the ground, 'Δ' shows the change of the snow pack SWE and 'P' the accumulated precipitation.

For the period from Feb. 21st to 23rd (at L2), both the observed precipitation and the assimilation results are much lower than the observed change (44 mm) in the SWE. On the other hand, if the snow pit data from Feb. 19th is considered, the SWE change is only 21 mm, which agrees with the assimilation results.

For the period from Feb. 21st to 22nd (at L1) the assimilation system overestimates the ΔSWE by 5.6 mm and from Feb. 22 to 24, the assimilation underestimates the change by 8.7 mm; still the results appear to be better than the observed precipitation, for which the observed snowfall was lower by 6.6 and 13.4 mm.

Only for the period between Feb. 23rd and Feb. 25th, the assimilation results were much worse than the observed precipitation; the system strongly overestimates the snowfall. Comparing 'A1' and 'A2' for 'L2' shows that 'A2' seems to provide a little bit better results for the period between Feb. 23rd and Feb. 25th. In this case, the observed brightness temperature change does not correspond to the results from the radiative transfer model. This might indicate a problem with the radiative transfer model and further investigation needs to be carried out to analyze the results.

DISCUSSION & OUTLOOK

The application of JMA-SiB to the CLPX data showed good results for the land-surface model for the snow conditions in Fraser. Good agreement was achieved for all parameters except temperature. For the two selected cases, the observed snow pack temperature is underestimated; one possible reason for this is that JMA-SiB does not consider the effect of the snow micro-structure on the thermal conductivity of the snow. The error in the snow temperature may be the reason for the slight overestimation of the snow grain size. By improving the estimation of the thermal conductivity, the representation of the snow temperature can be improved, which might lead to an improved representation of the snow micro-structure. Further work needs to be done to analyze the heat transfer in the snow pack.

The estimated amount of new snow from the assimilation is, with the exception of one case, closer to the SWE change in the snow pack, than the observed precipitation data. One problem can be changes in the new snow, from previous assimilation steps, during the assimilation period.

The current system only uses the TB data at 89 GHz but current satellite systems also provide observations at lower frequencies: for example, 18.7, and 36.5 GHz (AMSR-E). The lower frequencies are not sensitive to new snow and, therefore, can be used independent of the new snow assimilation system. In this case, attention to the snow metamorphism is necessary, and an important step was made by introducing the snow grain growth.

ACKNOWLEDGMENTS

This study was carried out as part of the Coordinated Enhanced Observing Period (CEOP) and Verification Experiment for AMSR/AMSR-E funded by the Japanese Science and Technology Corporation for Promoting Science and Technology Japan and the Japan Aerospace Exploration Agency. The authors express their great gratitude to them.

Furthermore, we would like to thank the National Aeronautics and Space Administration for providing us with the opportunity to participate in the CLPX, Don Cline for his great efforts in organizing the CLPX and also Janet Hardy who managed the LSOS.

REFERENCES

1. Rango, A., Walker, A.E. and Goodison, B. : Snow & Ice, Remote Sensing in Hydrology and Water Management,

Schultz, G. and Engman, E.T. eds., Springer Verlag, 2000.

2. Foster, J.L. and Rango, A. : Snow cover conditions in the northern hemisphere during the winter of 1981, Journal of Climatology, Vol.20, pp.171-183, 1982.
3. Steppuhn, H. : Snow and Agriculture, Handbook of Snow: Principles, Processes, Management and use, Gray, D.M. and Male D.N. eds., Pergamon Press, pp.60-125, 1981.
4. Allison, I., Barry, R.G. and Goodison, B.E. : Climate and cryosphere (CLiC) project science and co-ordination plan - Version 1, Technical Report WCRP-114, WMO/TD No.1053, World Climate Research Program, World Meteorological Organization, 2001.
5. Schmugge, T.J., Kustas, W.P., Ritchie, J.C., Jackson, T.J. and Rango, A. : Remote sensing in hydrology, Advances in Water Resources, Vol.25, pp.1367-1385, 2002.
6. Graf, T., Koike, T. and Nishimura, K. : Correcting solid precipitation from gauge observations using passive microwave brightness temperature data, Annual Journal of Hydraulic Engineering, Vol.48, JSCE, pp.259-264, 2004.
7. Pathmathevan, M., Koike, T., Li, X. and Fujii, H. : A simplified land data assimilation scheme and its application to soil moisture experiments in 2002 (SMEX02), Water Resources Research, Vol.39 (12), 2003
8. Hirai, M., Sakashita, T. and Matsumura, T. : Evaluation of a new land surface model for JMA-GSM - using CEOP EOP-3 reference site dataset, Proc. CEOP/IGWCO Joint Meeting, The University of Tokyo, pp.45-48, 2005.
9. Sellers, P.J., Mintz, Y., Sud, Y.C. and Dalcher, A. : A simple biosphere model (SiB) for use within general circulation models, Journal of Atmospheric Sciences, Vol.43(6), pp.505-531, 1986.
10. Jordan, R: A One-Dimensional temperature model for snow cover, Special Report 91-16, USACE-CRREL, 2001.
11. Wiesmann, A. and Mätzler, C. : Microwave emission model of layered snowpacks, Remote Sensing of Environment, Vol.70, pp.307-316, 1999.
12. Mätzler, C. and Wiesmann, A. : Extension of the microwave emission model of layered snowpacks to coarse-grained snow, Remote Sensing of Environment, Vol.70, pp.317-325, 1999.
13. Jin, Y.-Q. : Electromagnetic scattering modelling for quantitative remote sensing, World Scientific, 1994.
14. Courtier, P. : Variational methods, Journal of the Meteorological Society of Japan, Vol. 75, pp.211-218, 1997.
15. Duan, Q., Sorooshian, S., Gupta, V. : Effective and efficient global optimization for conceptual rainfall-runoff Models, Water Resources Research, Vol.28(4), pp.1015-1031, 1992.
16. Graf, T., Koike T., Fujii, H., Brodzik, M. and Armstrong, R. : CLPX-Ground: Ground based passive microwave radiometer (GBMR-7) Data, Boulder, CO, National Snow and Ice Data Center, Digital Media, 2003.
17. Hardy, J., Pomeroy, J., Link, T., Marks, D., Cline, D., Elder, K., Davis, R. : CLPX-Ground: Snow measurements at the local scale observation Site (LSOS), Boulder, CO, National Snow and Ice Data Center, Digital Media, 2003.
18. Cline, D., Armstrong, R., Davis, R., Elder, K. and Liston, G. : NASA Cold Land Processes Field Experiment Plan 2001-2004, http://www.nohrsc.nws.gov/~cline/clpx.html, 2001.
19. Hardy, J., Cline, D., Elder, K., Davis, R., Armstrong, R., Graf, T., Koike, T., DeRoo, R., Sarabandi, K., Castres Saint-Martin, G., Koh, G., Marshall, H-P., McDonald, K. and Painter, T. : An overview of data from the local scale observation site of the cold land processes experiment (CLPX), to be submitted to Journal of Hydrometeorology.
20. Lehning, M., Bartelt, P., Brown, B., Fierz, C. and Satyawali, P. : A physical SNOWPACK model for the swiss avalance warning. Part II. Snow microstructure, Cold Regions Science and Technology, Vol.35, pp.147-167, 2002.
21. Yamazaki, T. : A one-dimensional land surface model adaptable to intensely cold regions and its application in eastern Siberia, Journal of the Meteorological Society of Japan, Vol.79, pp.1107-1118, 2001.

APPENDIX – NOTATION

The following symbols are used in this paper:

c	= correction factor for observed snowfall;
$C_{i,t}$	= variation of saturation vapor pressure with temperature relative to ice;
dr/dt	= snow grain growth;
dT/dz	= temperature gradient in the snow pack;
D_{eos}	= effective diffusion coefficient of water vapor in snow;
f	= forcing data for model operator;
g_1, g_2	= empirical coefficients for snow grain growth model;
H	= observation operator or radiative transfer model;
J	= cost function;
J_B	= background error;
J_0	= observation error;
M	= model operator or land surface model;
P_a	= pressure of air;
r	= radius of snow grain;
R	= error covariance matrix of the observations;
SWE	= actual snow water equivalent;
SWE_g	= snow water equivalent observed by precipitation gauge;
T	= temperature of the snow pack;
T_0, T_1	= time before and after snowfall event;
TB_0, TB_1	= observed brightness temperature at T_0 and T_1;
$TB_{0,c}$, $TB_{1,c}$	= model estimated brightness temperature at T_0 and T_1;
x_0	= vector of initial conditions for model operator;
y_i^0	= vector of satellite observations; and
θ_l	= snow wetness.

(Received July 27, 2006 ; revised November 30, 2006)